HHS Public Access

Author manuscript

Biol Psychiatry. Author manuscript; available in PMC 2016 June 15.

Published in final edited form as:

Biol Psychiatry. 2015 June 15; 77(12): 1098–1107. doi:10.1016/j.biopsych.2015.01.020.

Delta frequency optogenetic stimulation of a thalamic nucleus reuniens is sufficient to produce working memory deficits; relevance to schizophrenia

Aranda R. Duan[*], **Carmen Varela**[‡], **Yuchun Zhang**[*], **Yinghua Shen**[‡], **Lealia Xiong**[‡], **Matthew Wilson**[‡], and **John Lisman**[*,•]

[*]Brandeis University, 415 South Street, Waltham, MA 02453

[‡]Massachusetts Institute of Technology, The Picower Institute for Learning and Memory, MIT Building 46-5233, 43 Vassar Street, Cambridge, MA 02139

Abstract

Background—Low-frequency (delta/theta) oscillations in the thalamocortical system are elevated in schizophrenia during wakefulness and are also induced in the NMDAR hypofunction rat model. To determine whether abnormal delta oscillations might produce functional deficits, we used optogenetic methods in awake rats. We illuminated channelrhodopsin-2 in the thalamic nucleus reuniens (RE) at delta frequency and measured the effect on working memory performance (the RE is involved in working memory (WM), a process affected in schizophrenia (SZ)).

Methods—We injected RE with a virus (AAV) to transduce cells with channelrhodopsin-2. An optical fiber was implanted just dorsal to the hippocampus in order to illuminate RE axon terminals.

Results—During optogenetic delta frequency stimulation, rats displayed a strong WM deficit. On the following day, performance was normal if illumination was omitted.

Conclusions—The optogenetic experiments showed that delta frequency stimulation of a thalamic nucleus is sufficient to produce deficits in WM. This result supports the hypothesis that delta frequency bursting in particular thalamic nuclei has a causal role producing WM deficits in this SZ. The action potentials in these bursts may jam communication through the thalamus, thereby interfering with behaviors dependent on WM. Studies in thalamic slices using the NMDAR hypofunction model show that delta frequency bursting is dependent on T-type Ca^{2+}

•Correspondence: John Lisman, Department of Biology, Volen Center for Complex Systems, Brandeis University, 415 South St., Waltham, MA 02454. Tel.no.:781-736-3148.

Financial Disclosure

The remaining authors reported no biomedical financial interests or potential conflicts of interest.

channels, a result that we confirmed here *in vivo*. These channels, which are strongly implicated in SZ by GWAS studies, may thus be a therapeutic target for treatment of SZ.

Keywords

schizophrenia; reuniens; delta; thalamus; optogenetics; channelrhodopsin

Introduction

Low-frequency cortical oscillations in the delta/theta range have abnormally high power in schizophrenia (SZ) patients in the awake (resting) state, a finding confirmed by EEG and MEG meta-analyses (1, 2). Delta oscillations occur globally during slow-wave sleep, but abnormal delta in SZ occurs in subregions of the thalamocortical system (medial prefrontal cortex, mPFC, and temporal lobes) (3). Elevated delta is present in un-medicated, first-episode patients (4–9) and thus cannot be attributed to drug treatment. Though there are some discrepancies, many studies have correlated the magnitude of delta elevation with both positive and negative symptoms of SZ (6, 10–13). Importantly, elevated delta correlates closely with the manifestation of the disease itself; increased delta power is observed in SZ patients, but not in healthy “at risk” subjects such as first-degree relatives (14–17). Even in twins discordant for SZ, increased delta power is not observed in the healthy twin (18, 19). This correlation with the disease stands in contrast to the gamma oscillation abnormality in SZ, which is present in relatives that do not have the disease (16, 20, 21). Thus, the gamma abnormality appears to be a predisposition for developing the disease (22), whereas the delta abnormality could be a direct cause.

A further connection between abnormal delta and SZ comes from studies using the NMDA hypofunction model of SZ (23–26), a model based on the observation that normal subjects develop both positive and negative symptoms of SZ in response to NMDAR antagonist (27–30). NMDAR antagonist produces delta oscillations in both animal models and humans (31–36), again raising the possibility that these oscillations might have a role in producing symptoms of SZ.

In this study, we sought to use an animal model to evaluate the hypothesis that abnormal delta oscillations can have a causal role in producing functional deficits, as previously suggested (37, 38). Although elevated delta correlates with SZ symptoms, as noted above, correlation is not proof. Ketamine and other NMDAR antagonists at high but subanesthetic doses induce delta oscillations in animals and humans (31–34, 36), and this is accompanied by aspects of psychosis (27–30, 39, 40). However, NMDAR antagonists also cause other changes, notably alteration in gamma oscillations (41–44). The role of delta in causing behavioral deficits therefore cannot be firmly established by these experiments. Thus, the fundamental question of whether abnormal delta oscillations can have a role in producing functional abnormalities remains unanswered.

To address this question, we have used optogenetics, a method that allows specific activity patterns to be induced in a defined set of cells. Using this method, we tested whether delta frequency stimulation of the nucleus reuniens of the thalamus (RE) interferes with working memory, a function that has deficits in schizophrenia (45). We targeted channelrhodopsin to

RE because this thalamic nucleus interconnects the mPFC and hippocampus, both of which are required for working and contextual memory (46–51), and because lesioning of RE interferes with working memory (46, 52–55).

A second goal of the current study relates to the cellular and molecular mechanisms that underlie abnormal delta oscillations. Use of the NMDA hypofunction model has provided mechanistic insight into this mechanism. The source of these oscillations appears to be the thalamus because NMDAR antagonist injected into the rat thalamus can evoke delta oscillations in the thalamus, which then are communicated to the cortex (31) and hippocampus (36). Experiments using a slice preparation of the thalamic reticular nucleus (TRN), an inhibitory pacemaker of the thalamus, have revealed that NMDAR antagonists block the NR2C channels prevalent in this structure (35). These channels generate a basal inward current due to ambient glutamate and can contribute to resting potential (NR2C channels, unlike NR2A and NR2B, are not blocked by Mg^{2+} at resting voltage (56, 57)). The blockade of this basal inward current causes hyperpolarization of the cells and thereby removes the inactivation from T-type Ca^{2+} channels (58). The T-type Ca^{2+} channels then generate Ca^{2+} spikes that trigger bursts of Na^{+} spikes at delta frequency. This bursting can produce delta frequency modulation of synaptic targets in the relay nuclei of the thalamus (59), and these cells, in turn, can drive delta modulation of their targets in the hippocampus (36) and cortex (31). We previously showed that thalamic delta oscillations induced by NMDAR antagonists can be reduced by antagonists of T-type Ca^{2+} channels and D2 receptors, but these results were obtained in a slice preparation (35). In the current paper, we sought to extend these results by testing whether these antagonists are also effective *in vivo*.

Methods and Materials

All experimental protocols were approved by the institutional animal care and use committees at Massachusetts Institute of Technology and Brandeis University.

Subjects

Male Long-Evans rats (Charles River, Wilmington, MA) were housed under a 12 h light/dark cycle in a temperature- and humidity-controlled environment with free access to food and water.

Surgery

For optogenetic experiments (Figures 1–3): Anesthesia was induced by intraperitoneal injection of ketamine (25 mg/kg), xylazine (3 mg/kg), and atropine (0.027 mg/kg), followed by maintenance with 1–2% inhaled isoflurane. A glass pipette (~60 μm in tip diameter) was connected to a stereotactic injector (Stoelting QSI injector) and filled with purified, concentrated adeno-associated virus, serotype 5 (~10^{12} infectious units ml^{-1}) encoding ChR2(H134R)-EYFP under control of the αCaMKII promoter (AAV5-CaMKIIa-hChR2(H134R)-EYFP from UNC Vector Core Services, Chapel Hill, NC). The coordinates of the injection site were 2.0 mm posterior to the bregma and 1.8 mm lateral to the midline. The injecting pipette was 16° oblique to the vertical line to avoid the midline blood vessel and sinus and was advanced 6.8 mm from the brain surface. 0.8 μl AAV vector was injected

at a rate of 0.1 μl per minute. After the injection was completed, the pipette was kept in its position for 15 minutes before slowly extracting. For fiber optic implantation in the hippocampus, the coordinates of the craniotomy were 4.0 mm posterior to bregma and 3.5 mm lateral to the midline. An optic fiber of known light transmittance was advanced 2.3 mm from the brain surface. In pilot experiments, there was variation in the coordinates of the injection site and of the fiber optic implant; furthermore, channelrhodopsin expression was not always immunohistologically verified but was always observed in the animals that were checked. Several bone screws were implanted for mechanical support, and the fiber and the screws were fixed to the skull with dental acrylic. The viral vector injection and fiber optic implantation occurred within the same surgery, and their locations were confirmed by examination of brain sections. The rats were given ≥4 weeks to recover before diet change and behavioral training ensued. Optogenetic stimulation occurred ≥6 weeks after surgery.

Surgery

For electrophysiology experiments (Figures 4–5): Rats were anesthetized using an intraperitoneal injection of ketamine/xylazine/acepromozine mixture (100, 5.2, and 1 mg/kg, respectively), with supplemental intraperitoneal injections administered as needed. Each anesthetized rat was placed in a standard stereotactic device, where its scalp was excised, and holes were bored in its skull for the insertion of 5–6 ground screws and electrode bundles. Multielectrode bundles (32 μm nichrome microwires) were inserted into dorsal hippocampal CA1 regions (rostral-caudal: −4.1 mm to bregma; medial-lateral: 2.5 mm to midline; dorsalventral: 2 mm to brain surface) or RE (rostral-caudal: −1.8 mm to bregma; medial-lateral: 1.0 mm to midline; dorsal-ventral: 6.8 mm to brain surface; 10° to vertical line). For local drug injection into the RE, a 27-G guiding cannula was implanted to guide a 30-G injecting cannula. Once in place, the assemblies were cemented to the skull. Rats were given 2 weeks to recover from the surgery and to get familiar with the recording environments. Rats were 2.5 months old at surgery and were about 3 months old at recording.

Electrophysiological recording and data analysis

The signal from each electrode was split: one channel (for spikes) was filtered at 300 to 5,000 Hz and sampled at 40,000 Hz; the other channel used to measure local field potentials (LFP) was filtered at 0.1 to 200 Hz and sampled at 1,000 Hz. Plexon software was used for data recording and storage. Spikes (and the delta phase of spikes) were analyzed as (36).

Histology

For optogenetic experiments (Figures 1–3): Rats were perfused according to standard protocol ≥8 weeks post surgery, and extracted brains were stored in 1× phosphate buffered solution (PBS) at 4°C, following a 12 hour submersion in 4% paraformaldehyde at 4°C. 60 μm sections were sliced on a Leica VT1000 S, and all sections between bregma −0.26 mm and bregma −5.20 mm, according to The Rat Brain Atlas in Stereotaxic Coordinates 2nd Ed. by Paxinos and Watson, were collected for YFP immunostaining. Briefly, slices were washed in PBS and placed in 10% methanol/ 3.5% hydrogen peroxide/ PBS for 1 hour at room temperature. Following PBS washes, the slices were placed in PBS/ 1% Triton/ 10% normal goat serum (PBST/NGS) for 2 hours at room temperature (Vector Laboratories, Inc.

NGS Cat# S-1000, Burlingame, CA). Slices were then placed in PBST/NGS with a 1:5,000 dilution of anti-chicken GFP primary antibody overnight at 4°C (a negative control was run for each rat in which the slices did not receive any primary antibody) (Aves Labs, Inc. Anti-GFP antibody, Chicken IgY 10 mg/mL Cat# GFP-1010, Tigard, OR). On the following day, slices were washed in PBS and placed in PBST/NGS with a 1:350 dilution of goat anti-chicken Alexa488 secondary antibody for 2 hours at room temperature (Life Technologies Alexa Fluor 488 goat anti-chicken IgG 2mg/mL Ref# A11039, Grand Island, NY). After a last round of PBS washes, slices were mounted onto microscope slides using Vectashield mounting medium with DAPI and coverslipped (Vector Laboratories, Inc. Vectashield Cat# H-1200, Burlingame, CA). Slices were viewed on a Zeiss Imager.M2, and images were captured with a Hamamatsu digital camera C10600 and processed with Zen 2012 software.

Histology

After the experimental sessions (Figures 4–5), rats were deeply anesthetized, 7 seconds of DC current (7 μA) were passed through selected microwires to mark the position of those electrodes, and then the animals were perfused through the heart with saline followed by 10% formalin in saline. Brains were removed and immersed in a sucrose formalin mixture, where they remained, refrigerated, until fixed. Sections (40 μm) cut through the implanted areas on a freezing microtome were stained with Prussian blue for ferrous deposits blasted off of the electrode tips and were counterstained with cresyl violet for cell bodies.

Behavior

At a minimum of 4 weeks postsurgery, animals were food restricted to approximately 85% of their *ad libitum* weight. The animals were given ~3 days to habituate to the T-maze, and then trained on a delayed alteration spatial WM task. The task was organized into trials having two runs. In the first run, rats ran from the starting box down the central arm of the maze and were prevented from entering one of the goal arms by a barrier (sample phase). Entry into the other arm was rewarded with 3–5 food pellets. In the second run, which occurred after a 15 second delay in the start box, the rats again ran down the central arm but had to choose between two open goal arms (choice phase). To obtain reward, animals were required to enter the goal arm not visited during the sample phase (two minutes between trials). 15 trials, or a total time of 75 minutes, were given to each animal daily (for one animal, there were only 10 trials [see Rat 1 in Figure 3]) until the animals could persist and complete 15 trials each day; on average, animals completed training by 2 weeks. A laser illuminated the fiber optic implant (200 μm) through a patch cord during testing. The laser intensity was 10–20 mW (wavelength 473 nm) controlled by a pulse generator (3 Hz; 100 ms on, 233 ms off). During testing, laser stimulation was on for the duration of the two runs of a trial (throughout the running, reward deliveries, and time interval between the two runs) and was turned off between trials. During testing, the animals completed all 15 trials, and their accuracy of performance was recorded. Wilcoxon-Mann-Whitney one-tailed U tests were run on the behavioral data to test for statistical significance.

Drug application

T-type Ca^{2+} channel blocker TTA-P2 was a gift from Merck. 1% TTA-P2 was prepared with 15% beta-cyclodextrin, and pH was adjusted to 7.0 with sodium hydroxide. TTA-P2 was injected intraperitoneally at 10 mg/kg. D2 antagonist was purchased from Sigma and was injected intraperitoneally at 1 mg/kg. For local ketamine injection into the RE, 1.5 μl ACSF containing 6 μg ketamine was injected into RE at a rate of 1 μl/min.

Results

Effects of optogenetic delta stimulation on working memory

At the start of these experiments, rats were injected with rAAV5-CaMKIIa-ChR2(H134R)-eYFP targeted to the RE (Figure 1A). The region transduced by the virus included both the RE and nearby thalamic nuclei (Figure 1C). Rats were also implanted with an optical fiber, the tip of which was just dorsal to the hippocampal CA1 region (Figure 1B). After several weeks, YFP was evident in the stratum lacunosum moleculare of CA1, the termination field of the RE in the hippocampus (Figure 1D). The fiber optic tip placement allowed for preferential activation of the RE axons in the hippocampus. Because RE is the only thalamic nucleus that innervates the hippocampal region (50, 60–62), this optogenetic strategy selectively excited cells of the RE that innervate the hippocampus.

Beginning at a minimum of 5 weeks post surgery, rats were trained on a hippocampal-dependent WM task (63). In the protocol utilized, each trial consisted of two runs in which the rat traveled along a central arm of a T-maze to the choice point and then traveled along one of the maze's arms. In the first run, the rat could only travel along a predetermined arm (randomly chosen) at the choice point and was always rewarded. In the second run (initiated 15 seconds later), the rat was free to choose which arm to enter and was rewarded only if the arm chosen was opposite to that on the previous run (i.e., to alternate). The rats achieved 15 trials per day and learned to alternate over approximately 2 weeks of training (Figure 2A). Individual rats were considered fully trained when the rat made ≥90% correct choices for at least 3 consecutive training days (Figure 2B).

We then determined whether delta frequency illumination of the RE terminals could disrupt performance in this WM task. An illumination frequency of 3 Hz (100 ms on; 233 ms off) was chosen to match the frequency of delta frequency modulation of the RE evoked by systemic ketamine injection (Figure 1E shows the delta frequency local field potential and the delta frequency modulation of spike phase). Such illumination was given during the entire trial (both runs and the delay period). During illumination, rats completed all 15 trials, with no obvious change in motivation. However, delta frequency illumination produced a substantial reduction in the percent of correct choices (from 0.94 ± 0.05 to 0.69 ± 0.08, n=3, $P<0.05$, Figure 2B, Day T1). A subsequent set of trials on the following day was done without illumination; under these conditions, no performance deficit was observed (0.92 ± 0.02, n=3, Figure 2B, Day T2). In the next set of trials (Day T3), illumination was again given and again produced a reduction in performance (0.82 ± 0.04, n=3, $P<0.05$, Figure 2B, Day T3). On Day T4, rats were again tested without illumination and showed normal performance (1.00 ± 0.00, n=2, Figure 2B, Day T4). The rats were sacrificed for

immunostaining and demonstrated expression of channelrhodopsin (Figure 2C; five pilot experiments were done without verification of expression by immunostaining, and these gave similar results, as described in the Fig. 2C caption).

Light activation of channelrhodopsin has now been used in many types of experiments, and there has been no indication that illumination can itself affect behavior (64). To ensure that this is also the case in our experiments, we trained a group of animals that had been injected with saline instead of virus. After rats made ≥90% correct choices for 3 consecutive training days, we tested the effect of delta frequency illumination and found no effect on either Day T1 or Day T3 (from 0.96 ± 0.04 to 0.98 ± 0.04 on Day T1, $P>0.1$, and from 1.00 ± 0.00 to 0.96 ± 0.04 on Day T3, $P>0.1$, $n = 3$) (Figure 3).

Effects of drugs on delta oscillations induced by ketamine injection into RE

We previously showed in a slice preparation that antagonists of T-type Ca^{2+} channels and D2 receptors block the delta frequency bursting of rat TRN neurons induced by NMDAR antagonist (35). To determine whether the delta oscillations induced *in vivo* and transmitted to the hippocampus have a similar pharmacology, we measured delta oscillations in the field potential of CA1 hippocampal region induced by injection of ketamine into the RE, a structure with excitatory input to CA1 (61, 62, 65). These injections were done in the awake state. Figure 4 (top) shows the tracks made by the guiding cannula (targeted at the RE) and by the recording electrode (targeted at the hippocampus). Similar to the experiments by Zhang *et al*. (36), local injection of ketamine (6 μg in 1.5 μl) into the RE induced a dramatic increase in delta power in the hippocampus (183% ± 23% of pre-ketamine) (Figure 4). The delta observed in the hippocampal local field potential is not simply volume conducted from elsewhere but reflects activity in the hippocampus, as evidenced by the fact that action potentials of hippocampal neurons during ketamine are phase locked to the hippocampal delta oscillations in the field potential (36).

We measured the effect of D2 antagonist or T-type Ca^{2+} channel antagonist on these oscillations. The D2 antagonist haloperidol was intraperitoneally injected 10 minutes prior to local ketamine infusion in the RE. Under these conditions, ketamine failed to induce an increase in delta power (103% ± 5% of pre-haloperidol level; $n = 6$) (Figure 5 B,D).

We next measured the effect of systemically applied TTA-P2, a specific T-type Ca^{2+} channel antagonist (66). Ten minutes later, ketamine was injected. TTA-P2 completely blocked the ketamine-induced delta oscillations (Fig. 5C,D; 98% ± 5% of pre-TTA-P2, $n = 6$).

Discussion

Although the abnormality in delta oscillations in SZ is well established (1, 2), it has been unclear whether this abnormality would be expected to have deleterious functional consequences. We have therefore done experiments in rats to determine whether optogenetic stimulation at a delta frequency in a small thalamic nucleus (RE) that is involved in WM is sufficient to interfere with WM function. Our results show that strong WM deficits are produced, thus lending support to the hypothesis (37, 38) that low-frequency oscillations in

subregions of the thalamus are causal in producing symptoms of SZ. One caveat, however, must be noted: the above hypotheses that we have tested assume that in SZ, as in NMDAR hypofunction models and sleep, a large fraction of cells in the affected nuclei are active at delta frequency, an activity that could interfere with information processing. Proof of this assumption awaits cellular recordings from patients.

The fact that WM deficits can be produced by interfering with RE function is consistent with previous work demonstrating the importance of RE in the delayed alternation WM task (46, 49, 50, 54, 65). Specifically, recent experiments suggest that RE brings information about the previous trial to the hippocampus (47, 67). In our experiments, stimulation was present during both the encoding and the retrieval phases of the task; further work will be required to determine whether RE is important during one or both phases.

We can only speculate about the mechanism by which delta interferes with WM. Oscillations in the field potential are generated by the synchronized firing of neurons. In the thalamus, this firing is generated by long spikes produced by T-type Ca^{2+} channels, which, in turn, trigger bursts of Na^{+} spikes (35, 58); this bursting repeats at delta frequency. Such delta frequency activity can be easily observed (e.g., Figure 1E) and so must occur in a large fraction of neurons. One possibility is that the delta evoked in the thalamus disrupts downstream hippocampal function, which depends on theta and gamma oscillations (48, 68–72). However, another possibility, which we consider very likely, is that the repetitive delta frequency firing “jams” the transmission of WM information through the thalamus; specifically, abnormal delta frequency bursting in relay cells is likely to interfere with the normal signal carrying WM information. From this perspective, what produces the jamming is the presence of repetitive firing in a large fraction of cells; the exact frequency of this firing may not be important. In SZ, it so happens that delta frequency bursting is what occurs. The important point established by our results is that such a signal, even when evoked in a small part of the thalamus, is sufficient to produce a deficit in WM.

Evidence for abnormal function of the thalamus in SZ

Several lines of evidence point to thalamic dysfunction in SZ (73–86), but methods to identify deficits in RE are not yet available. One indirect line of evidence consistent with an abnormality in RE comes from high-resolution studies of basal blood volume. These studies show a form of hypermetabolism in CA1, but not in other hippocampal fields. This hypermetabolism correlates with symptomology (30, 40, 87). Because RE is the only thalamic nucleus to innervate CA1 and because CA1 is the only hippocampal region to receive thalamic input, delta frequency bursting in RE neurons could potentially account for the specific hypermetabolism of CA1 (50, 61, 62).

Several lines of evidence point to the idea that some regions of the brain may become functionally disconnected in SZ (3, 25, 88–91). Emerging evidence in human studies suggests that disconnection may prevent corollary discharge signals generated in the frontal lobes from reaching the temporal lobe (90). It has been argued that interference with corollary discharge could lead to positive symptoms of SZ, in which the sense of self is disturbed (92). Because there are indications that corollary discharge is transmitted via the thalamus (93, 94), the possibility should be considered that delta oscillations in certain

thalamic nuclei jam information flow and thereby produce the disconnection that impedes the flow of corollary discharge.

Potential pharmacological approaches for treatment of SZ

We showed previously that D2 antagonist depolarizes TRN cells in a slice preparation, a depolarization that inactivates T-type Ca^{2+} channels (35), leading to a cessation of delta frequency bursting. Here we report that the D2 antagonist is also effective in blocking the delta oscillations induced *in vivo* by ketamine injection into RE. This effect may be due to D2 antagonist action on the RE. Notably, D2 antagonist has been shown to increase counts of cFOS-positive interneurons in midline thalamic nuclei (including RE) (95). Excitation of these interneurons could inhibit RE relay cells and thereby prevent delta generation. However, we cannot exclude a more complex scenario in which the D2 antagonist acts on the TRN.

We showed previously that T-type Ca^{2+} channel antagonist (TTA-P2) blocks delta oscillations in a slice preparation. Here we show that this antagonist blocks the delta oscillations induced *in vivo* by ketamine injection into RE. These results suggest that T-type Ca^{2+} channels may be important in SZ. Indeed, large-scale genome-wide association studies have identified the CACNA1I T-type Ca^{2+} channel gene as a risk factor in SZ (96, 97). Another line of recent work also points in this direction. It was shown that ethosuximide, a drug that blocks T-type Ca^{2+} channels, can block the elevated low-frequency oscillations in a SZ mouse model and reverse cognitive impairments (98). Thus, blocking delta oscillations using T-type Ca^{2+} channel antagonists may have a therapeutic effect in schizophrenia. There has been one controlled study that evaluated T-type Ca^{2+} channel antagonist as a treatment for SZ, but this study was a “failed study” (there was no effect beyond placebo of either D2 or T-type Ca^{2+} channel antagonist) (99). Further investigation of the therapeutic potential of T-type Ca^{2+} channel antagonists is therefore warranted.

Acknowledgments

We thank the National Institutes of Health for funding our research, and we thank the Lisman lab and the Wilson lab group members for insightful discussion. This work was supported by the NIH grant numbers R01MH086518-05 and T32NS007292-28 and R01-GM104948-02.

John Lisman received an honorarium from Pfizer Pharmaceuticals in Cambridge, Massachusetts for a lecture he gave in December 2013. He also receive an honorarium from Roche Pharmaceuticals for a lecture he gave at the Roche Innovation Center in Basel, Switzerland in September 2014.

References

1. Boutros NN, Arfken C, Galderisi S, Warrick J, Pratt G, Iacono W. The status of spectral EEG abnormality as a diagnostic test for schizophrenia. Schizophrenia research. 2008; 99:225–237. [PubMed: 18160260]
2. Siekmeier PJ, Stufflebeam SM. Patterns of spontaneous magnetoencephalographic activity in patients with schizophrenia. J Clin Neurophysiol. 2010; 27:179–190. [PubMed: 20461010]
3. Schulman JJ, Cancro R, Lowe S, Lu F, Walton KD, Llinas RR. Imaging of thalamocortical dysrhythmia in neuropsychiatry. Frontiers in human neuroscience. 2011; 5:69. [PubMed: 21863138]
4. Harris A, Melkonian D, Williams L, Gordon E. Dynamic spectral analysis findings in first episode and chronic schizophrenia. Int J Neurosci. 2006; 116:223–246. [PubMed: 16484051]

5. John JP, Rangaswamy M, Thennarasu K, Khanna S, Nagaraj RB, Mukundan CR, et al. EEG power spectra differentiate positive and negative subgroups in neuroleptic-naive schizophrenia patients. J Neuropsychiatry Clin Neurosci. 2009; 21:160–172. [PubMed: 19622687]
6. Kirino E. Mismatch negativity correlates with delta and theta EEG power in schizophrenia. Int J Neurosci. 2007; 117:1257–1279. [PubMed: 17654091]
7. Morihisa JM, Duffy FH, Wyatt RJ. Brain electrical activity mapping (BEAM) in schizophrenic patients. Arch Gen Psychiatry. 1983; 40:719–728. [PubMed: 6860073]
8. Pascual-Marqui RD, Lehmann D, Koenig T, Kochi K, Merlo MC, Hell D, et al. Low resolution brain electromagnetic tomography (LORETA) functional imaging in acute, neuroleptic-naive, first-episode, productive schizophrenia. Psychiatry Res. 1999; 90:169–179. [PubMed: 10466736]
9. Sponheim SR, Clementz BA, Iacono WG, Beiser M. Resting EEG in first-episode and chronic schizophrenia. Psychophysiology. 1994; 31:37–43. [PubMed: 8146253]
10. Begic D, Mahnik-Milos M, Grubisin J. EEG characteristics in depression, "negative" and "positive" schizophrena. Psychiatr Danub. 2009; 21:579–584. [PubMed: 19935497]
11. Fehr T, Kissler J, Moratti S, Wienbruch C, Rockstroh B, Elbert T. Source distribution of neuromagnetic slow waves and MEG-delta activity in schizophrenic patients. Biological psychiatry. 2001; 50:108–116. [PubMed: 11526991]
12. Fehr T, Kissler J, Wienbruch C, Moratti S, Elbert T, Watzl H, et al. Source distribution of neuromagnetic slow-wave activity in schizophrenic patients--effects of activation. Schizophrenia research. 2003; 63:63–71. [PubMed: 12892859]
13. Gschwandtner U, Zimmermann R, Pflueger MO, Riecher-Rossler A, Fuhr P. Negative symptoms in neuroleptic-naive patients with first-episode psychosis correlate with QEEG parameters. Schizophrenia research. 2009; 115:231–236. [PubMed: 19683895]
14. Clementz BA, Sponheim SR, Iacono WG, Beiser M. Resting EEG in first-episode schizophrenia patients, bipolar psychosis patients, and their first-degree relatives. Psychophysiology. 1994; 31:486–494. [PubMed: 7972603]
15. Sponheim SR, Iacono WG, Thuras PD, Nugent SM, Beiser M. Sensitivity and specificity of select biological indices in characterizing psychotic patients and their relatives. Schizophrenia research. 2003; 63:27–38. [PubMed: 12892855]
16. Venables NC, Bernat EM, Sponheim SR. Genetic and disorder-specific aspects of resting state EEG abnormalities in schizophrenia. Schizophr Bull. 2009; 35:826–839. [PubMed: 18381357]
17. Hong LE, Summerfelt A, Mitchell BD, O'Donnell P, Thaker GK. A shared low-frequency oscillatory rhythm abnormality in resting and sensory gating in schizophrenia. Clinical neurophysiology : official journal of the International Federation of Clinical Neurophysiology. 2012; 123:285–292. [PubMed: 21862398]
18. Stassen HH, Coppola R, Gottesman II, Torrey EF, Kuny S, Rickler KC, et al. EEG differences in monozygotic twins discordant and concordant for schizophrenia. Psychophysiology. 1999; 36:109–117. [PubMed: 10098386]
19. Weisbrod M, Hill H, Sauer H, Niethammer R, Guggenbuhl S, Hell D, et al. Nongenetic pathologic developments of brain-wave patterns in monozygotic twins discordant and concordant for schizophrenia. Am J Med Genet B Neuropsychiatr Genet. 2004; 125B:1–9. [PubMed: 14755436]
20. Hall MH, Taylor G, Salisbury DF, Levy DL. Sensory Gating Event-Related Potentials and Oscillations in Schizophrenia Patients and Their Unaffected Relatives. Schizophr Bull. 2010
21. Hall M-H, Taylor G, Sham P, Schulze K, Rijsdijk F, Picchioni M, et al. The early auditory gamma-band response is heritable and a putative endophenotype of schizophrenia. Schizophrenia bulletin. 2011; 37:778–787. [PubMed: 19946013]
22. Lisman JE, Pi HJ, Zhang Y, Otmakhova NA. A thalamo-hippocampal-ventral tegmental area loop may produce the positive feedback that underlies the psychotic break in schizophrenia. Biological psychiatry. 2010; 68:17–24. [PubMed: 20553749]
23. Coyle JT, Balu D, Benneyworth M, Basu A, Roseman A. Beyond the dopamine receptor: novel therapeutic targets for treating schizophrenia. Dialogues Clin Neurosci. 2010; 12:359–382. [PubMed: 20954431]
24. Javitt DC, Zukin SR. Recent advances in the phencyclidine model of schizophrenia. Am J Psychiatry. 1991; 148:1301–1308. [PubMed: 1654746]

25. Marek GJ, Behl B, Bespalov AY, Gross G, Lee Y, Schoemaker H. Glutamatergic (N-methyl-D-aspartate receptor) hypofrontality in schizophrenia: too little juice or a miswired brain? Molecular pharmacology. 2010; 77:317–326. [PubMed: 19933774]
26. Moghaddam B, Krystal JH. Capturing the angel in "angel dust": twenty years of translational neuroscience studies of NMDA receptor antagonists in animals and humans. Schizophr Bull. 2012; 38:942–949. [PubMed: 22899397]
27. Coyle JT. Glutamate and schizophrenia: beyond the dopamine hypothesis. Cellular and Molecular Neurobiology. 2006; 26:365–384. [PubMed: 16773445]
28. Krystal JH, D'Souza DC, Mathalon D, Perry E, Belger A, Hoffman R. NMDA receptor antagonist effects, cortical glutamatergic function, and schizophrenia: toward a paradigm shift in medication development. Psychopharmacology. 2003; 169:215–233. [PubMed: 12955285]
29. Krystal JH, Karper LP, Seibyl JP, Freeman GK, Delaney R, Bremner JD, et al. Subanesthetic effects of the noncompetitive NMDA antagonist, ketamine, in humans. Psychotomimetic, perceptual, cognitive, and neuroendocrine responses. Arch Gen Psychiatry. 1994; 51:199–214. [PubMed: 8122957]
30. Schobel SA, Chaudhury NH, Khan UA, Paniagua B, Styner MA, Asllani I, et al. Imaging patients with psychosis and a mouse model establishes a spreading pattern of hippocampal dysfunction and implicates glutamate as a driver. Neuron. 2013; 78:81–93. [PubMed: 23583108]
31. Buzsaki G. The thalamic clock: emergent network properties. Neuroscience. 1991; 41:351–364. [PubMed: 1870695]
32. Dimpfel W, Spuler M. Dizocilpine (MK-801), ketamine and phencyclidine: low doses affect brain field potentials in the freely moving rat in the same way as activation of dopaminergic transmission. Psychopharmacology. 1990; 101:317–323. [PubMed: 2163537]
33. Miyasaka M, Domino EF. Neural mechanisms of ketamine-induced anesthesia. Int J Neuropharmacol. 1968; 7:557–573. [PubMed: 5753175]
34. Palenicek T, Fujakova M, Brunovsky M, Balikova M, Horacek J, Gorman I, et al. Electroencephalographic Spectral and Coherence Analysis of Ketamine in Rats: Correlation with Behavioral Effects and Pharmacokinetics. Neuropsychobiology. 2011; 63:202–218. [PubMed: 21422767]
35. Zhang Y, Llinas RR, Lisman JE. Inhibition of NMDARs in the nucleus reticularis of the thalamus produces delta frequency bursting. Frontiers in Neural Circuits. 2009; 3:20. [PubMed: 20057928]
36. Zhang Y, Yoshida T, Katz DB, Lisman JE. NMDAR antagonist action in thalamus imposes delta oscillations on the hippocampus. Journal of neurophysiology. 2012; 107:3181–3189. [PubMed: 22423006]
37. Llinas RR, Ribary U, Jeanmonod D, Kronberg E, Mitra PP. Thalamocortical dysrhythmia: A neurological and neuropsychiatric syndrome characterized by magnetoencephalography. Proceedings of the National Academy of Sciences of the United States of America. 1999; 96:15222–15227. [PubMed: 10611366]
38. Sharp FR, Hendren RL. Psychosis: atypical limbic epilepsy versus limbic hyperexcitability with onset at puberty? Epilepsy Behav. 2007; 10:515–520. [PubMed: 17416210]
39. Lodge DJ, Grace AA. The hippocampus modulates dopamine neuron responsivity by regulating the intensity of phasic neuron activation. Neuropsychopharmacology. 2006; 31:1356–1361. [PubMed: 16319915]
40. Small SA, Schobel SA, Buxton RB, Witter MP, Barnes CA. A pathophysiological framework of hippocampal dysfunction in aging and disease. Nature Review Neuroscience. 2011; 12:585–601.
41. Faulkner HJ, Traub RD, Whittington MA. Disruption of synchronous gamma oscillations in the rat hippocampal slice: a common mechanism of anaesthetic drug action. British journal of pharmacology. 1998; 125:483–492. [PubMed: 9806331]
42. Hong LE, Summerfelt A, Buchanan RW, O'Donnell P, Thaker GK, Weiler MA, et al. Gamma and delta neural oscillations and association with clinical symptoms under subanesthetic ketamine. Neuropsychopharmacology : official publication of the American College of Neuropsychopharmacology. 2010; 35:632–640. [PubMed: 19890262]
43. Mann EO, Mody I. Control of hippocampal gamma oscillation frequency by tonic inhibition and excitation of interneurons. Nat Neurosci. 2010; 13:205–212. [PubMed: 20023655]

44. McNally JM, McCarley RW, Brown RE. Chronic Ketamine Reduces the Peak Frequency of Gamma Oscillations in Mouse Prefrontal Cortex Ex vivo. Front Psychiatry. 2013; 4:106. [PubMed: 24062700]
45. Forbes NF, Carrick LA, McIntosh AM, Lawrie SM. Working memory in schizophrenia: a meta-analysis. Psychological medicine. 2009; 39:889–905. [PubMed: 18945379]
46. Hallock HL, Wang A, Shaw CL, Griffin AL. Transient inactivation of the thalamic nuclues reuniens and rhomboid nucleus produces deficits of a working-memory dependent tactile-visual conditional discrimination task. Behavioral Neuroscience. 2013; 127:860–866. [PubMed: 24341710]
47. Ito, HT.; Zhang, SJ.; Witter, MP.; Moser, EI.; Moser, MB. Trajectory-dependent firing in hippocampal place cells reflects nucleus reuniens-mediated input from the medial prefrontal cortex. National Institute for Physiological Sciences International Symposium; Norwegian University of Science and Technology; 2013.
48. Jones MW, Wilson MA. Theta rhythms coordinate hippocampal-prefrontal interactions in a spatial memory task. PLoS Biol. 2005; 3:e402. [PubMed: 16279838]
49. Prasad, JA.; Chudasama, Y. Spatial working memory impairment following selective lesions of the thalamic reuniens; Society for Neuroscience Conference; 2013. 575.516/JJJ563.
50. Vertes RP, Hoover WB, Szigeti-Buck K, Leranth C. Nucleus reuniens of the midline thalamus: link between the medial prefrontal cortex and the hippocampus. Brain research bulletin. 2007; 71:601–609. [PubMed: 17292803]
51. Xu W, Sudhof TC. A neural circuit for memory specificity and generalization. Science. 2013; 339:1290–1295. [PubMed: 23493706]
52. Davoodi F, Motamedi F, Akbari E, Ghanbarian E, Jila B. Effect of reversible inactivation of reuniens nucleus on memory processing in passive avoidance task. Behavioural brain research. 2011; 221:1–6. [PubMed: 21354215]
53. Hembrook J, Onos K, Mair R. Inactivation of ventral midline thalamus produces selective spatial delayed conditional discrimination impairment in the rat. Hippocampus. 2012; 22:853–860. [PubMed: 21542055]
54. Hembrook JR, Mair RG. Lesions of reuniens and rhomboid thalamic nuclei impair radial maze win-shift performance. Hippocampus. 2011; 21:815–826. [PubMed: 20572196]
55. Loureiro M, Cholvin T, Lopez J, Merienne N, Latreche A, Cosquer B, et al. The ventral midline thalamus (reuniens and rhomboid nuclei) contributes to the persistence of spatial memory in rats. The Journal of neuroscience. 2012; 32:9947–9959. [PubMed: 22815509]
56. Monyer H, Sprengel R, Schoepfer R, Herb A, Higuchi M, Lomeli H, et al. Heteromeric NMDA receptors: molecular and functional distinction of subtypes. Science. 1992; 256:1217–1221. [PubMed: 1350383]
57. Sah P, Hestrin S, Nicoll RA. Tonic activation of NMDA receptors by ambient glutamate enhances excitability of neurons. Science. 1989; 246:815–818. [PubMed: 2573153]
58. Llinas RR, Steriade M. Bursting of thalamic neurons and states of vigilance. Journal of neurophysiology. 2006; 95:3297–3308. [PubMed: 16554502]
59. Yu E, Choi S, Lisman JE, Llinas RR. Block of NMDA receptors in the thalmic reticular nucleus produces abnormal thalamocortical rhythms. Frontiers. (submitted).
60. Varela C, Kumar S, Yang JY, Wilson MA. Anatomical substrates for direct interactions between hippocampus, medial prefrontal cortex, and the thalamic nucleus reuniens. Brain Structure and Function. 2014; 219:911–929. [PubMed: 23571778]
61. Vertes RP, Hoover WB, Do Valle AC, Sherman A, Rodriguez JJ. Efferent projections of reuniens and rhomboid nuclei of the thalamus in the rat. J Comp Neurol. 2006; 499:768–796. [PubMed: 17048232]
62. Wouterlood FG, Saldana E, Witter MP. Projection from the nucleus reuniens thalami to the hippocampal region: light and electron microscopic tracing study in the rat with the anterograde tracer Phaseolus vulgaris-leucoagglutinin. J Comp Neurol. 1990; 296:179–203. [PubMed: 2358531]

63. Maruki K, Izaki Y, Hori K, Nomura M, Yamauchi T. Effects of rat ventral and dorsal hippocampus temporal inactivation on delayed alternation task. Brain research. 2001; 895:273–276. [PubMed: 11259790]
64. Liu X, Ramirez S, Pang PT, Puryear CB, Govindarajan A, Deisseroth K, et al. Optogenetic stimulation of a hippocampal engram activates fear memory recall. Nature. 2012; 484:381–385. [PubMed: 22441246]
65. Ito, HT.; Moser, EI.; Moser, M-B. Society for Neuroscience Meeting. Washington, D.C.: 2011. Representation of behavioral context in the nucleus reuniens for CA1 place cells.
66. Dreyfus FM, Tscherter A, Errington AC, Renger JJ, Shin HS, Uebele VN, et al. Selective T-type calcium channel block in thalamic neurons reveals channel redundancy and physiological impact of I(T)window. The Journal of neuroscience : the official journal of the Society for Neuroscience. 2010; 30:99–109. [PubMed: 20053892]
67. Ito HT, Witter EI, Moser EI, Moser MB. Representation of behavioral context in the nucleus reuniens for CA1 place cells. Society for Neuroscience. 2012
68. Hyman JM, Zilli EA, Paley AM, Hasselmo ME. Medial prefrontal cortex cells show dynamic modulation with the hippocampal theta rhythm dependent on behavior. Hippocampus. 2005; 15:739–749. [PubMed: 16015622]
69. Hyman JM, Zilli EA, Paley AM, Hasselmo ME. Working Memory Performance Correlates with Prefrontal-Hippocampal Theta Interactions but not with Prefrontal Neuron Firing Rates. Frontiers in Integrative Neuroscience. 2010; 4:1–13. [PubMed: 20161992]
70. Lisman J, Buzsáki G. A Neural Coding Scheme Formed by the Combined Function of Gamma and Theta Oscillations. Schizophrenia Bulletin. 2008; 34:974–980. [PubMed: 18559405]
71. Siapas AG, Lubenov EV, Wilson MA. Prefrontal phase locking to hippocampal theta oscillations. Neuron. 2005; 46:141–151. [PubMed: 15820700]
72. Yamamoto J, Suh J, Takeuchi D, Tonegawa S. Successful execution of working memory linked to synchronized high-frequency gamma oscillations. Cell. 2014; 157:845–857. [PubMed: 24768692]
73. Andreasen NC. The role of the thalamus in schizophrenia. Canadian journal of psychiatry Revue canadienne de psychiatrie. 1997; 42:27–33. [PubMed: 9040920]
74. Andreasen NC, Arndt S, Swayze V 2nd, Cizadlo T, Flaum M, O'Leary D, et al. Thalamic abnormalities in schizophrenia visualized through magnetic resonance image averaging. Science. 1994; 266:294–298. [PubMed: 7939669]
75. Ben-Shachar D, Bonne O, Chisin R, Klein E, Lester H, Aharon-Peretz J, et al. Cerebral glucose utilization and platelet mitochondrial complex I activity in schizophrenia: A FDG-PET study. Prog Neuropsychopharmacol Biol Psychiatry. 2007; 31:807–813. [PubMed: 17329000]
76. Brickman AM, Buchsbaum MS, Shihabuddin L, Byne W, Newmark RE, Brand J, et al. Thalamus size and outcome in schizophrenia. Schizophrenia research. 2004; 71:473–484. [PubMed: 15474918]
77. Buchsbaum MS, Someya T, Teng CY, Abel L, Chin S, Najafi A, et al. PET and MRI of the thalamus in never-medicated patients with schizophrenia. The American journal of psychiatry. 1996; 153:191–199. [PubMed: 8561198]
78. Byne W, Buchsbaum MS, Kemether E, Hazlett EA, Shinwari A, Mitropoulou V, et al. Magnetic resonance imaging of the thalamic mediodorsal nucleus and pulvinar in schizophrenia and schizotypal personality disorder. Arch Gen Psychiatry. 2001; 58:133–140. [PubMed: 11177115]
79. Clinton SM, Meador-Woodruff JH. Thalamic dysfunction in schizophrenia: neurochemical, neuropathological, and in vivo imaging abnormalities. Schizophrenia research. 2004; 69:237–253. [PubMed: 15469196]
80. Coscia DM, Narr KL, Robinson DG, Hamilton LS, Sevy S, Burdick KE, et al. Volumetric and shape analysis of the thalamus in first-episode schizophrenia. Human brain mapping. 2009; 30:1236–1245. [PubMed: 18570200]
81. Frazier JA, Hodge SM, Breeze JL, Giuliano AJ, Terry JE, Moore CM, et al. Diagnostic and sex effects on limbic volumes in early-onset bipolar disorder and schizophrenia. Schizophr Bull. 2008; 34:37–46. [PubMed: 18003631]

82. Hazlett EA, Buchsbaum MS, Kemether E, Bloom R, Platholi J, Brickman AM, et al. Abnormal glucose metabolism in the mediodorsal nucleus of the thalamus in schizophrenia. The American journal of psychiatry. 2004; 161:305–314. [PubMed: 14754780]
83. Malaspina D, Harkavy-Friedman J, Corcoran C, Mujica-Parodi L, Printz D, Gorman JM, et al. Resting neural activity distinguishes subgroups of schizophrenia patients. Biological psychiatry. 2004; 56:931–937. [PubMed: 15601602]
84. Popken GJ, Bunney WE Jr, Potkin SG, Jones EG. Subnucleus-specific loss of neurons in medial thalamus of schizophrenics. Proceedings of the National Academy of Sciences of the United States of America. 2000; 97:9276–9280. [PubMed: 10908653]
85. Shenton ME, Dickey CC, Frumin M, McCarley RW. A review of MRI findings in schizophrenia. Schizophrenia research. 2001; 49:1–52. [PubMed: 11343862]
86. Soyka M, Koch W, Moller HJ, Ruther T, Tatsch K. Hypermetabolic pattern in frontal cortex and other brain regions in unmedicated schizophrenia patients. Results from a FDG-PET study. Eur Arch Psychiatry Clin Neurosci. 2005; 255:308–312. [PubMed: 15834758]
87. Schobel SA, Lewandowski NM, Corcoran CM, Moore H, Brown T, Malaspina D, et al. Differential targeting of the CA1 subfield of the hippocampal formation by schizophrenia and related psychotic disorders. Arch Gen Psychiatry. 2009; 66:938–946. [PubMed: 19736350]
88. Anticevic A, Cole MW, Repovs G, Savic A, Driesen NR, Yang G, et al. Connectivity, pharmacology, and computation: toward a mechanistic understanding of neural system dysfunction in schizophrenia. Front Psychiatry. 2013; 4:169. [PubMed: 24399974]
89. Callicott JH, Mattay VS, Verchinski BA, Marenco S, Egan MF, Weinberger DR. Complexity of prefrontal cortical dysfunction in schizophrenia: more than up or down. The American journal of psychiatry. 2003; 160:2209–2215. [PubMed: 14638592]
90. Sigurdsson T, Stark KL, Karayiorgou M, Gogos JA, Gordon JA. Impaired hippocampal-prefrontal synchrony in a genetic mouse model of schizophrenia. Nature. 2010; 464:763–767. [PubMed: 20360742]
91. Tan HY, Callicott JH, Weinberger DR. Dysfunctional and compensatory prefrontal cortical systems, genes and the pathogenesis of schizophrenia. Cerebral cortex (New York, NY : 1991). 2007; 17(Suppl 1):i171–i181.
92. Ford JM, Mathalon DH, Whitfield S, Faustman WO, Roth WT. Reduced communication between frontal and temporal lobes during talking in schizophrenia. Biological psychiatry. 2002; 51:485–492. [PubMed: 11922884]
93. Sommer MA, Wurtz RH. What the brain stem tells the frontal cortex. II. Role of the SC-MD-FEF pathway in corollary discharge. Journal of neurophysiology. 2004; 91:1403–1423. [PubMed: 14573557]
94. Vukadinovic Z. Sleep abnormalities in schizophrenia may suggest impaired trans-thalamic cortico-cortical communication: towards a dynamic model of the illness. The European journal of neuroscience. 2011; 34:1031–1039. [PubMed: 21895800]
95. Ma J, Ye N, Lange N, Cohen BM. Dynorphinergic GABA neurons are a target of both typical and atypical antipsychotic drugs in the nucleus accumbens shell, central amygdaloid nucleus and thalamic central medial nucleus. Neuroscience. 2003; 121:991–998. [PubMed: 14580949]
96. Genome-wide association study implicates HLA-C*01:02 as a risk factor at the major histocompatibility complex locus in schizophrenia. Biol Psychiatry. 2012; 72:620–628. [PubMed: 22883433]
97. Biological insights from 108 schizophrenia-associated genetic loci. Nature. 2014; 511:421–427. [PubMed: 25056061]
98. Lee H, Dvorak D, Fenton AA. Targeting neural synchrony deficits is sufficient to improve cognition in a schizophrenia-related neurodevelopmental model. Frontiers in Psychiatry. 2014; 5:1–17. [PubMed: 24478729]
99. Egan MF, Zhao X, Smith A, Troyer MD, Uebele VN, Pidkorytov V, et al. Randomized controlled study of the T-type calcium channel antagonist MK-8998 for the treatment of acute psychosis in patients with schizophrenia. Hum Psychopharmacol. 2013; 28:124–133. [PubMed: 23532746]

100. McGuire PK, Silbersweig DA, Wright I, Murray RM, David AS, Frackowiak RS, et al. Abnormal monitoring of inner speech: a physiological basis for auditory hallucinations. Lancet. 1995; 346:596–600. [PubMed: 7651003]

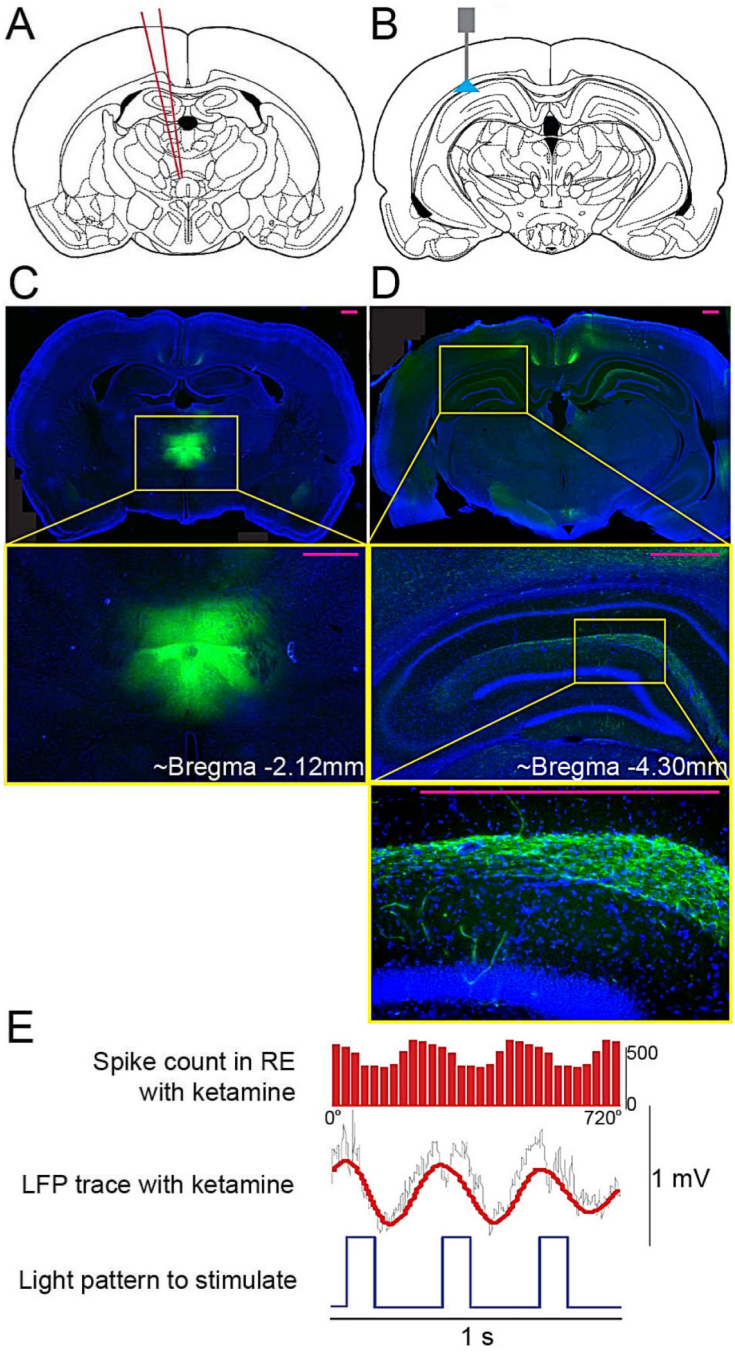

Figure 1.

Strategy of experiments to test whether delta frequency optogenetic stimulation of RE interferes with working memory (76). A. Schematic showing the site of the YFP-fused adeno-associated virus (AAV) injection in the midline thalamus, including the nucleus reuniens (RE) of the thalamus. B. Schematic showing the site of the fiber optic tip placed just above CA1, where it can selectively excite the RE axons in that region. C. Localization of AAV-mediated expression in the RE visualized by YFP immunostaining (shown in green; blue is DAPI nuclear staining). The virally induced expression spreads 1–2 mm. The RE is

located just above the third ventricle. D. Green shows YFP immunostaining of RE axons in CA1. E. Delta frequency activity in RE induced by systemic injection of ketamine. Top trace shows spike phase relative to delta oscillations in the local field potential of RE. Middle trace shows local field potential in RE (green, raw; red, filtered). Bottom trace shows pattern of delta frequency light stimulation (~3 Hz) used in the optogenetic experiments; data from the work of (36). Tissue shown was perfused 5 weeks post surgery to represent the expression level of injected virus at the time that animal behavior training would begin (n=2); calibration bars, 500 microns.

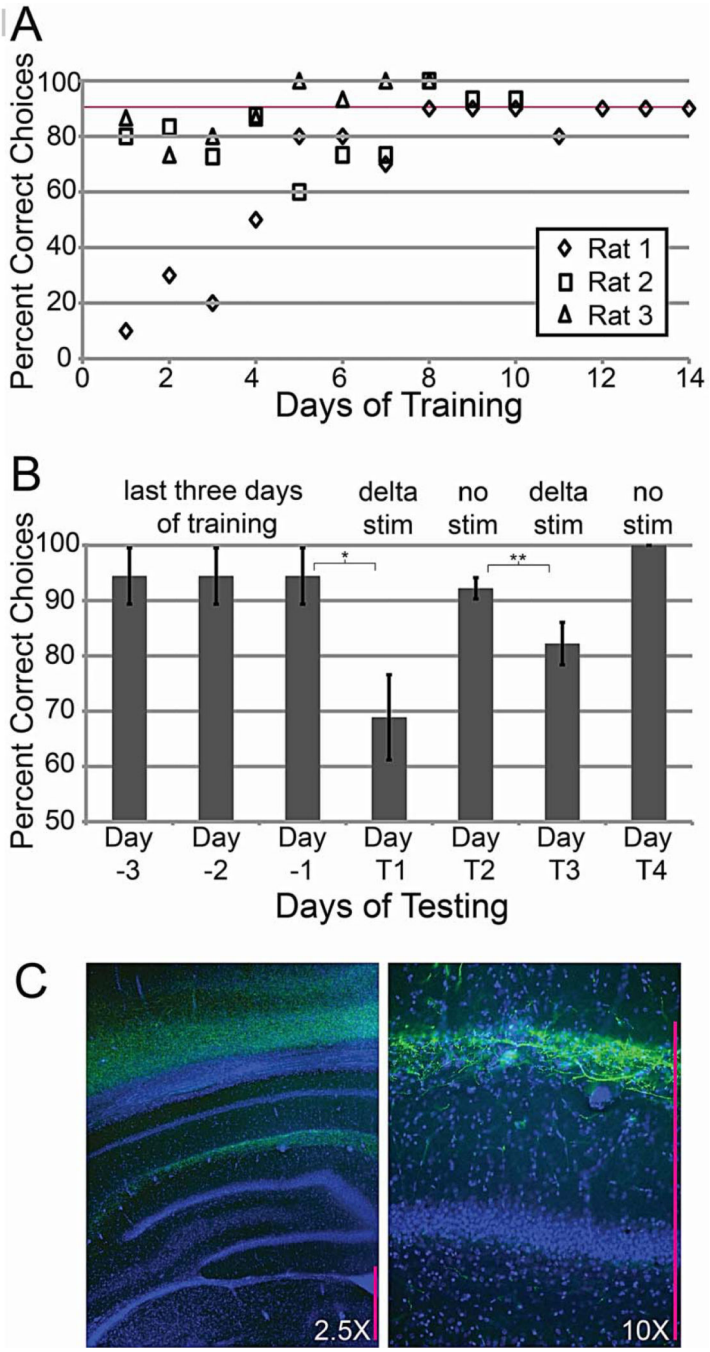

Figure 2.

Inducing delta oscillations in the nucleus reuniens (RE) is sufficient to interfere with the performance of a hippocampal-dependent, delayed alternation WM task. In this task, rats learned to alternate between the arms of a T-maze to receive a food reward. A. Rats were trained daily for up to 75 minutes or 15 trials until each individual rat could complete 15 trials per day. Each individual rat was considered fully trained upon completing 3 consecutive days of 15 trials each in which the rat made ≥90% correct (red line) choices (n=3). The below chance performance during early training is due to the fact that some rats

made systematic errors by going to previously rewarded arms of the maze (other rats tended to spontaneously alternate). B. Effect of delta frequency illumination of channelrhodopsin after training. Day 3 to Day 1 are the last 3 days of training in which the rats made ≥90% correct choices (n=3). On the first day of testing after training (Day T1), delta frequency illumination was given and performance dropped to 69% (n=3; $P<0.05$). The effect of light was evident in each animal (Rat 1: 0.90 to 0.60; Rat 2: 0.93 to 0.73; Rat 3: 1.00 to 0.73). On testing Day T2, rats were tested without illumination and behavior returned to normal (~92% correct; n=3; $P>0.1$). On testing Day T3, illumination was again given and performance dropped to about 82% (n=3; $P<0.05$). The effect of light was again evident in each animal (Rat 1: 0.90 to 0.80; Rat 2: 0.93 to 0.87; Rat 3: 0.93 to 0.80). On testing Day T4, the rats were once again tested without illumination and behavior returned to normal (100% correct; n=2; $P>0.1$; 473 nm laser intensity was 10–20 mW). In pilot experiments in which expression was not confirmed by immunostaining, consistent data was obtained in five additional animals; percentages of correct choices dropped from 0.96±0.05 to 0.72±0.08 on Day T1 and from 0.92±0.04 to 0.70±0.07 on Day T3 (data not shown; $P<0.05$). C. Rats were subsequently perfused, and YFP immunostaining was performed to demonstrate the expression levels of channelrhodopsin ≥5 months past DayT3; images show the hippocampus at ~bregma −3.80 mm; calibration bars, 500 microns; *$P<0.05$, **$P<0.05$.

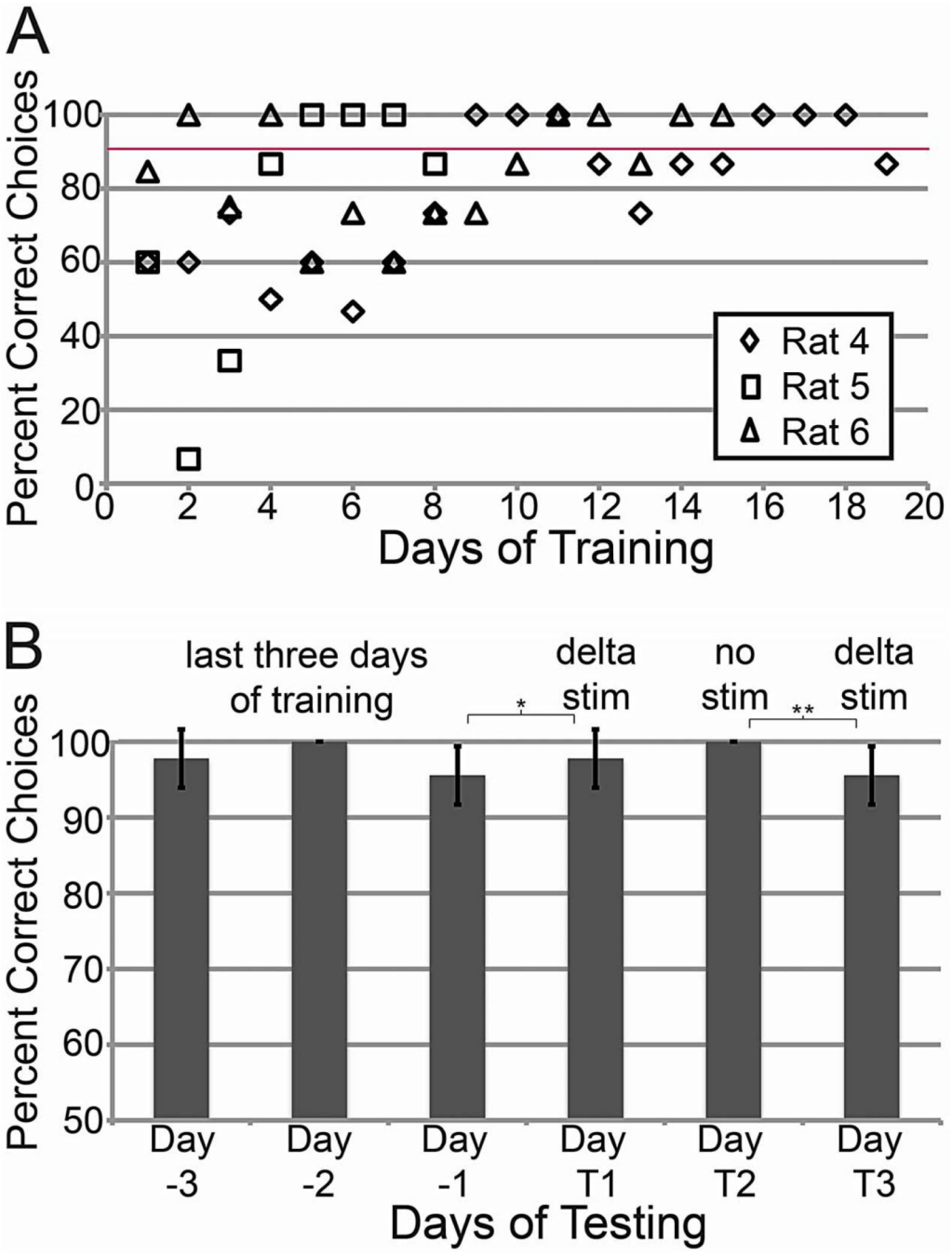

Figure 3.

Light stimulation had no effect in control animals injected with saline instead of the AAV virus. Rats were trained daily as described in Figure 1 until each individual rat completed 3 consecutive days of 15 trials each in which the rat made ≥90% (red line) correct choices (n=3). Day 3 to Day 1 are the last 3 days of training in which the rats made ≥90% correct choices. The rats received delta frequency illumination on testing Day T1, no illumination on Day T2, and delta illumination again on Day T3. No change in behavior was observed with illumination in these control animals (Day T1: 0.93 to 1.00 for Rat 1, 0.93 to 0.93 for

Rat 2, 1.00 to 1.00 for Rat 3; Day T3: 1.00 to 0.93 for Rat 1, 1.00 to 1.00 for Rat 2, 1.00 to 0.93 for Rat 3). *P>0.1, **P>0.1.

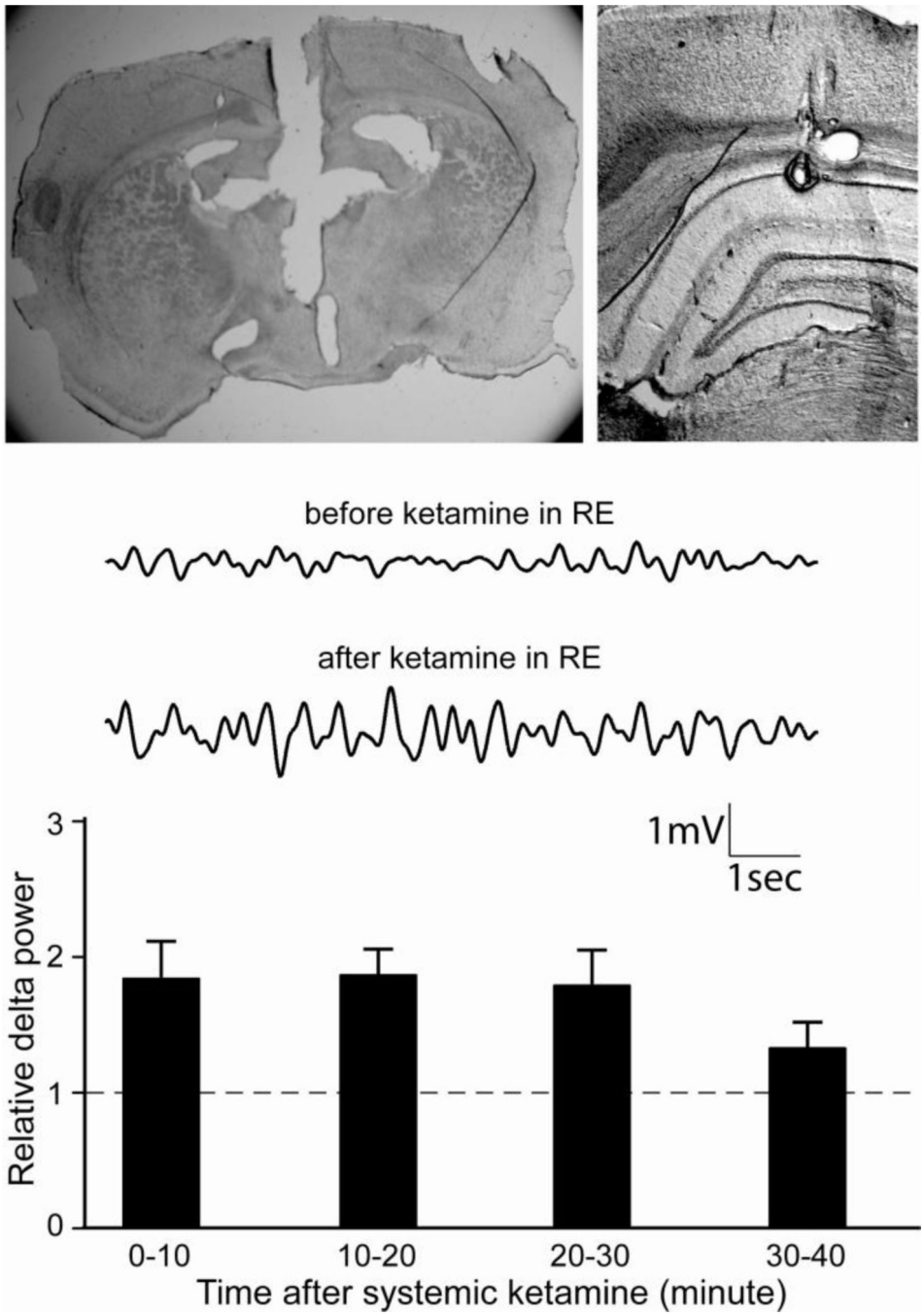

Figure 4.

Local ketamine injection into the nucleus reuniens (RE) of the thalamus induced delta oscillation in the hippocampus. A. Sections showing the site of ketamine injection near the RE (left) and the site of a recording electrode in CA1 pyramidal cell layer (100). B. (Top) Local field potential in CA1 before and after ketamine injection in the RE. (Bottom) Relative increase in hippocampal delta power at various times after ketamine injection.

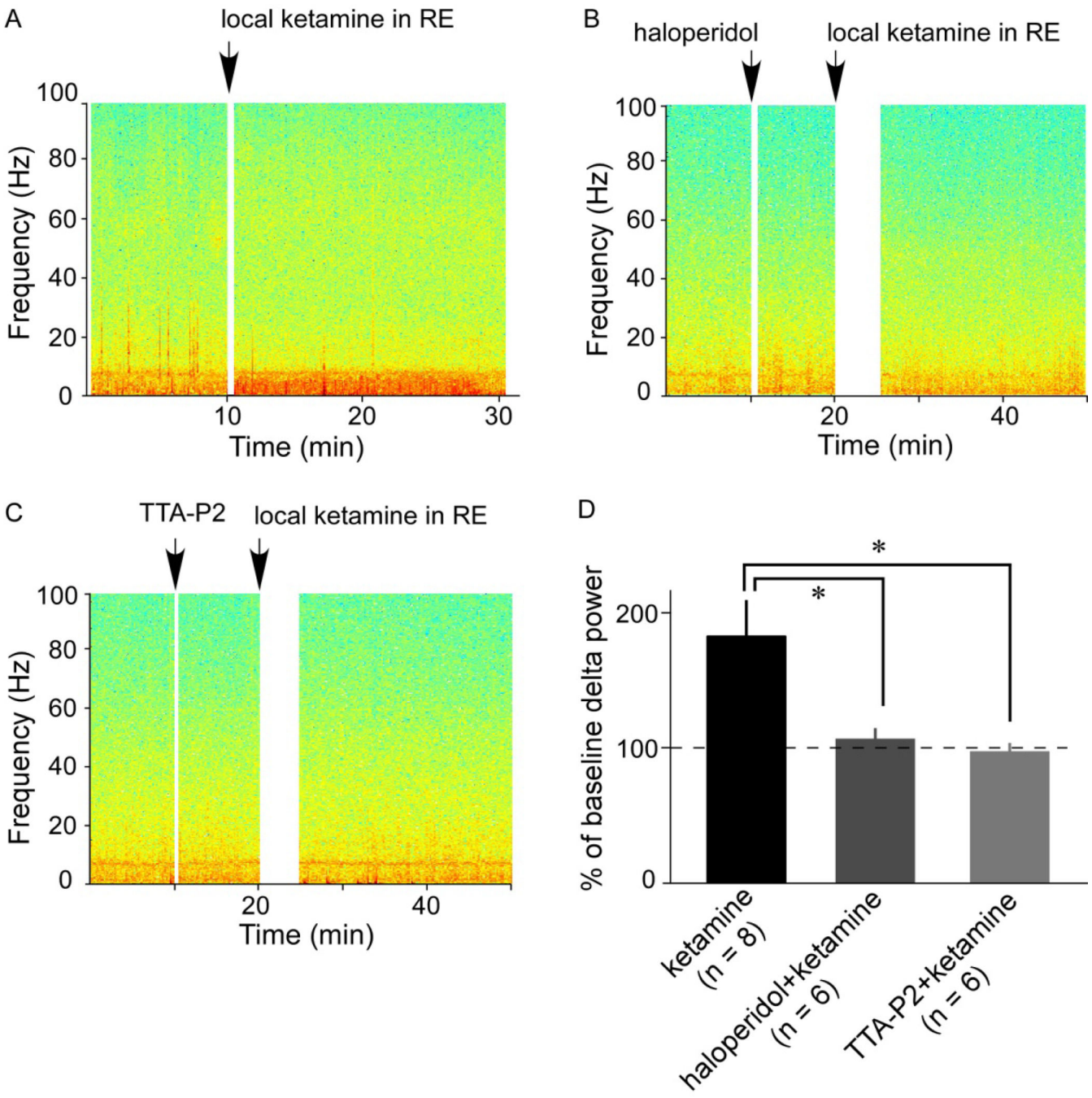

Figure 5.

Haloperidol and TTA-P2 blocked the delta oscillations in the hippocampus induced by ketamine injection into RE. A. Time course of oscillation power at different frequencies before and after ketamine injection into the RE. There is an increase in power in the delta range after ketamine injection. B. The increase in delta power is blocked by prior systemic injection of haloperidol. C. The increase in delta power is blocked by prior systemic

injection of the T-type Ca^{2+} channel antagonist, TTA-P2. D. Bar graph summary of the data (*P<0.05).